Environ. Sci. Technol. **1999**, *33,* 1840−1846

Instrumental Analysis Study of Iron Species Biosorption by *Sargassum* Biomass

M. M. FIGUEIRA,† B. VOLESKY,*,‡ AND H. J. MATHIEU§

Department of Chemical Engineering, McGill University, 3610 University St. Montreal, Quebec, Canada H2A 2B2, Ph.D. Program in Metallurgical and Mining Engineering, Federal University of Minas Gerais, Belo Horizonte, Brazil, and LMCH/Departement des Materiaux, EPFL, Lausanne, Switzerland

The mechanism of iron uptake by the dry biomass of the brown seaweed *Sargassum fluitans* was investigated at the molecular level using different instrumental techniques. Transmission electron microscopy (TEM) and the chemical microanalysis by electron dispersive spectroscopy (EDS) of the biomass exposed to iron solutions confirmed the deposition of the metal mainly in the cell wall. The analysis of the Fe(II)-exposed biomass by X-ray photoelectron spectroscopy (XPS) indicated the presence of Fe in two states of oxidation in the biomass exposed to ferrous iron solution, whereas only Fe(III) was present in ferric iron-exposed biomass, suggesting a partial oxidation of Fe(II) when in contact with the biomass. In both Fe(II)- and Fe(III)-exposed samples, XPS indicated iron complexation with sulfate groups in the biomass. The FTIR analysis of metal-loaded biomass samples revealed the chelating character of the ion complexation to carboxyl groups as well as the complexation of Fe(III) with sulfur of sulfonate groups in the biomass. This work confirmed the participation of carboxyl groups in the uptake of both Fe(II) and Fe(III), and of sulfonate groups in the uptake of Fe(III) by *S. fluitans* biomass.

Introduction

The interaction of metals with biological materials has been investigated for several years. In fact, such interaction has been associated with metal-based staining for electron microscopy observations. In this case, differential staining is achieved by using the relative binding specificity of some metals for characteristic chemical groups in biological tissues. For example, bismuth binds to amino groups of basic proteins, and silver and ruthenium are used for detecting aldehyde groups of mucopolysaccharides and diffuse proteins (*1*).

The ability of some biological materials to sequester metals from solutions led to the development of biosorbents. Shumate and Strandberg (*2*) define biosorption as a non-directed physicochemical interaction that may occur between metal/radionuclide species and the cellular compounds of biological specimens. Many biomass types have been screened for their metal-sorption capacity (*3*). The promising utilization of biomaterials in the treatment of metal-bearing solutions is mainly due to their low costs and high efficiency of removing metals from wastewater containing low concentrations of heavy metals (*4*).

A very well studied biosorption system is the one utilizing biomass of the brown macroalga *Sargassum* as a biosorbent. The metal uptake can reach up to 40% of the biomass dry weight (*5*), and satisfactory results were obtained for the uptake of cadmium and copper using seaweed biomass in columns (*4*). The main mechanism involved in the metal accumulation by *Sargassum* is ion-exchange (*6*), at least in the case of gold and cadmium, with ions occupying carboxyl groups in the biomass (*5, 7*). The effect of iron on the biosorption of cadmium by *Sargassum* biomass was previously investigated, and the methodology established can be broadly used (*8*). This work also provided the basis for the biosorption process of removing heavy metals from iron-containing wastewater using continuous-flow sorption columns (*9*).

Transmission electron microscopy (TEM), coupled with a microanalysis apparatus such as the electron dispersive spectroscope (EDS), can provide a valuable input in determining the distribution of the metal−biomass binding throughout the cell structure. When the objective is to obtain structural as well as analytical information about the metal−biomass interactions, the Fourier transform infrared (FTIR) and the X-ray photoelectron (XPS) spectroscopies are very helpful, especially considering the simple sample preparation procedures. Infrared spectroscopy has proven to be a powerful tool for studying biological molecules, and its application in obtaining structural and bonding information on complex and large molecules has been fruitful (*10*). The possibility of studying surface chemistry of solids in a nondestructive manner by XPS analysis made it one of the most powerful analytical techniques available to chemists (*11*). The use of this technique to investigate the valence of a metal in metal-containing proteins (*12*) is just one example of its applications. Other information such as the nature of attachment of biomolecules to metallic surfaces can also be obtained by the means of XPS analysis (*13*).

While the quantitative evaluation of the experimental data indicated that ion exchange is also the main mechanism of iron uptake by *Sargassum* biosorbent, the chemical groups responsible for metal accumulation in the biomass still need to be firmly established. These aspects are the focus of the present work using more sophisticated instrumental analytical techniques.

Experimental Section

Experimental Biomass and Metal Loading Conditions. *Sargassum fluitans* was collected and sun-dried in Naples, Florida, in winter time. Particles (0.5−0.84 mm) of disintegrated raw biomass were protonated with 0.2 N H_2SO_4 followed by a rinse with distilled water until the pH of the solution reached the value of 4.5. The conversion of the protonated biomass to Ca biomass was carried out with a 1.2 g/L solution of $Ca(OH)_2$. The pH of spent wash solution was 6.5. Finally, the biomass was dried overnight and then used in the experiments.

Protonated biomass was used for TEM/EDS and FTIR studies, and Ca biomass was used for XPS and FTIR analyses. The main advantage of using Ca-loaded biomass is in the stability of the solution pH during sorption experiments, in contrast with protonated biomass which exchanges protons with the metal whereby the solution pH decreases as a result.

* Corresponding author. E-mail: boya@chemeng.lan.mcgill.ca.
† Federal University of Minas Gerais.
‡ McGill University.
§ EPF Lausanne.

10.1021/es981111p CCC: $18.00
Published on Web 04/21/1999

For the TEM/EDS studies, biomass particles (0.1 g) were contacted with 50 mL of a 5 mM Fe(II) solution (sulfate salt $FeSO_4 \cdot 7H_2O$). The contents of 125-mL Erlenmeyer flasks were adjusted to pH 4.5. After a 3-h experimental contact period on a shaker (3.3 Hz) at room temperature, the biomass was separated from the solution and dried for the electron microscopy preparation.

For XPS and FTIR analyses, biomass particles (0.02 g) were respectively contacted with 10 mL of 5 mM Fe(II) or Fe(III) (sulfate salts) solutions. The contents of tests tubes were adjusted to pH 4.0 and 2.0, respectively, to avoid precipitation of the metal. After 10 h of sorption contact under N_2 atmosphere (1 atm), the supernatant was discarded and the biomass was left to dry under N_2 atmosphere at 40 °C. This procedure was carried out in order to avoid any redox reactions in the solution that would not be due to the presence of the biomass. The concentration of ferrous Fe in the liquid samples was determined according to the Penny-Knop method (*14*) by titrating aliquots of samples with potassium dichromate. The total concentration of Fe was determined by atomic absorption spectroscopy (Thermo Jarrel Ash, model Smith-Hieftje II) and compared to that obtained for Fe (II). This procedure was carried out in order to confirm the concentrations of ferrous and ferric ions in solution.

Transmission Electron Microscopy/Electron Dispersive Spectroscopy Preparation. *Sargassum* biomass samples used for TEM/EDS were (i) previously pretreated with acid and (ii) contacted with the metal solution. Biomass particles were fixed by submerging them in 2.5% (w/v) glutaraldehyde−phosphate buffer for 2 h. The samples were washed repeatedly with 0.1 M phosphate buffer and dehydrated in a graded ethanol series (50 to 100%) and acetone (100%). Resin infiltration was carried out overnight in 2:1 (v/v) acetone/resin (*15*), then further 4 h in 1:1 (twice), and finally overnight in 100% resin. The resin infiltration steps were carried out at 20 °C, and eventually, the samples were transferred into molds filled with fresh Spurr resin for polymerization at 60 °C for 24 h. Thin sections were obtained using a Reichert-Jung Ultracut E ultramicrotome with diamond knives and mounted in 100 mesh aluminum grids. Sections were examined with a JEOL 4000FX transmission electron microscope in conjunction with an EDS detector. All sections were unstained. The voltage used was 80 kV for morphological observations and 120 kV for the EDS analysis; counts were accumulated over 300 s on at least 5 sections of each sample.

X-ray Photoelectron Spectroscopy Analysis. Samples for XPS analyses were prepared by attaching a very thin layer of freshly prepared powder to an adhesive tape placed on a sample holder. The XPS studies were carried out with a Perkin-Elmer PHI 5500 ESCA System, using monochromatic aluminum Kα ($E = 1486.6$ eV) radiation. An instrument vacuum of at least 10^{-9} Torr was mantained for all the analyses. The instrument was calibrated for $Au4f_{7/2}$ peak binding energy of 84.0 eV. All spectra were acquired with a resolution of 0.5 eV. The binding energies for the XPS spectra were referenced to the hydrocarbon component of the C1s spectrum at 285.0 eV. The XPS spectra were fit by using Gaussian−Lorentzian peak shapes, and Shirley's baseline correction function was subtracted.

Fourier-Transform Infrared Analysis. Infrared spectra of protonated or Ca- or Fe-loaded algal biomass were recorded on a Michelson 100 FTIR spectrophotometer. Disks of 100 mg of KBr containing 1% of finely ground powder (<20 mm) of each sample were prepared less than 24 h before recording.

Results

Electron Microscopy of Iron Adsorption. Transmission electron microscopy was used to examine samples of *Sargassum* biomass either exposed or not to iron solutions.

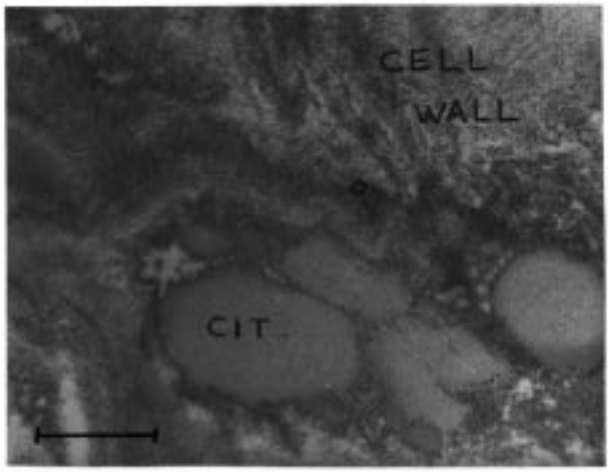

FIGURE 1. Transmission electron micrograph of *Sargassum* biomass exposed to a iron sulfate solution (bar = 0.1 μm).

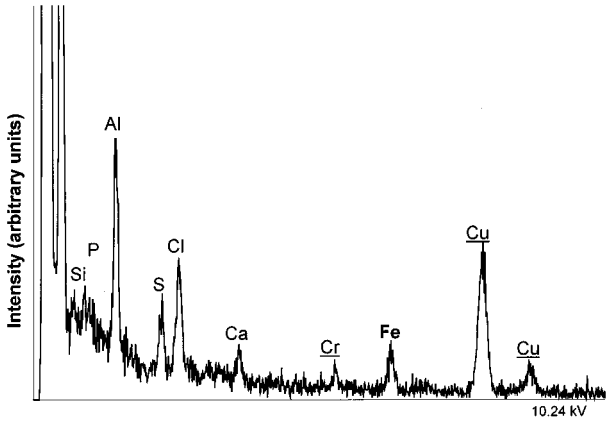

FIGURE 2. X-ray microanalysis spectrum of the cell wall of *Sargassum* thallus exposed to iron sulfate solution. Obs: underlined elements correspond to the background interference from the chemical composition of sample holder in the instrument.

Two regions of the seaweed plant were prepared for the TEM studies: thallus and blade. There was no major difference between those two plant segments in terms of iron deposition. A typical electron micrograph of *Sargassum* biomass after exposure to iron-containing solutions is presented in Figure 1. Iron deposition was obvious in the iron-exposed biomass examined by the transmission electron microscope. Morphological changes in the tissues, such as shrinking of the cellular contents and presence of "ghosts" inside the cell wall structures, were mainly due to their dehydration after collection and exposure to acids during the pretreatment procedure. Indeed, control samples of the biomass without metal (not shown) demonstrated the same lack of organization of the cell and only structures of the cell wall could be distinguished. Desiccation of plant tissues occurs rapidly after their removal from the plant, which causes changes at the ultrastructural level. It is known that, if the plant cell is killed before fixation, the compartmentalization pattern is lost because of the damage in vacuolar membranes (*16*).

The EDS analysis of the unstained sections of *Sargassum* confirmed the presence of Fe in the samples. Figure 2 represents the spectrum of X-ray microanalysis of the cell wall of the thallus. Similar spectra were obtained for the blade sections. Although Fe was mainly detected in the cell wall of *Sargassum* tissues, it was also present in the cytoplasmic and nuclear materials.

X-ray Photoelectron Spectroscopy Analysis. Experiments with *Sargassum* biomass for chemical information on the

TABLE 1: XPS Spectral Values of Binding Energy (eV) and Full Width at Half Maximum (FWHM) for Fitted Peaks of Fe(II)- and Fe(III)-Exposed *Sargassum* Samples

	Fe2p		Fe3p		S2p	
biomass	eV	FWHM	eV	FWHM	eV	FWHM
Fe(II)-exposed	709.9 ± 0.1	3.02	nd[a]	nd	168.2 ± 0.1	1.63
	723.1 ± 0.1	2.82			169.4 ± 0.1	1.83
					169.5 ± 0.1	1.60
					170.7 ± 0.1	1.33
Fe(III)-exposed	710.5 ± 0.1	2.90	56.2 ± 0.1	2.00	168.2 ± 0.1	1.80
	724.0 ± 0.1	2.77			169.4 ± 0.1	1.80
					169.3 ± 0.1	1.66
					170.5 ± 0.1	1.61

[a] nd: not determined.

interaction of iron with specific binding sites in the biomass were carried out with sulfate solutions of ferrous or ferric iron. It is not expected that ferrous species would rapidly oxidize under the experimental conditions (pH lower than 4.0 and under N_2 atmosphere) (*17*). The determination of ferrous content in $FeSO_4$ solution was carried out in order to confirm that it was not oxidized. Indeed, 98.2% of the total iron in solution (determined by AAS) was present as ferrous species. This information was important since any conclusion on the valence and speciation of iron in the biomass must consider the chemistry of the solution used. It was assumed that no chemical iron modification in the solution occurred under the experimental conditions.

The analysis of C1s bands for all of the samples revealed that only the Fe(III)-exposed biomass sample analyzed by XPS was electrically charged (shift of −1 eV). Table 1 shows the binding energy values and FWHM (full width at half-maximum) for Fe2p, Fe3p, and S2p of both samples analyzed. Figure 3, parts A and B, show the XPS Fe2p spectra for the *Sargassum* biomass samples exposed to ferrous and ferric iron, respectively. In both spectra the asymmetric bands for Fe ($2p^3/_2$) and Fe ($2p^1/_2$) are evident. For the sample exposed to Fe(III), the shape of the main Fe ($2p^3/_2$) line is clearly narrower, while the Fe ($2p^3/_2$) spectrum of the *Sargassum* biomass exposed to Fe(II) is broadened on the low binding energy side of the band. These same features are present in the Fe3p spectrum for Fe(III)-exposed biomass sample (Figure 4). In the spectra of Fe(II)-exposed biomass (Figure 3A) the low binding energy components are ascribed to the presence of ferrous iron (*18*). These results indicate the presence of Fe in two states of oxidation in the biomass exposed to ferrous iron solution, whereas only Fe(III) was present in ferric iron-exposed biomass, suggesting a partial oxidation of Fe(II) when in contact with the biomass.

Some differences were also observed in the spectra of S2p ($^3/_2$ and $^1/_2$) when both samples were compared. A broader band for Fe(II)-exposed samples was observed when compared to the one for Fe(III)-exposed biomass (Figure 5, parts A and B, respectively). Fitting showed that the envelope of the S2p is composed of 2 doublet peaks ($2p^3/_2$ and $2p^1/_2$) at 168.2 ± 0.1 and 169.4 ± 0.1 eV for the $2p^3/_2$ peaks. Peak separation between $2p^3/_2$ and $2p^1/_2$ is 1.18 eV which is in agreement with handbook data (*19*). These are values within the range of sulfonates and sulfate, respectively (*20*, *21*). This is the first evidence of specific iron complexation with sulfate groups in the biomass.

Fourier Transform Infrared Analysis. Infrared spectra of protonated or calcium- or iron-loaded *Sargassum* biomass samples are shown in Figure 6. The spectrum of protonated biomass typically displays absorbance peaks at 1738 cm^{-1} corresponding to the stretching band of the free carbonyl double bond from the carboxyl functional group. After the contact with Ca or Fe solutions, the biological material exhibited spectra with clear shifts of the carbonyl stretching

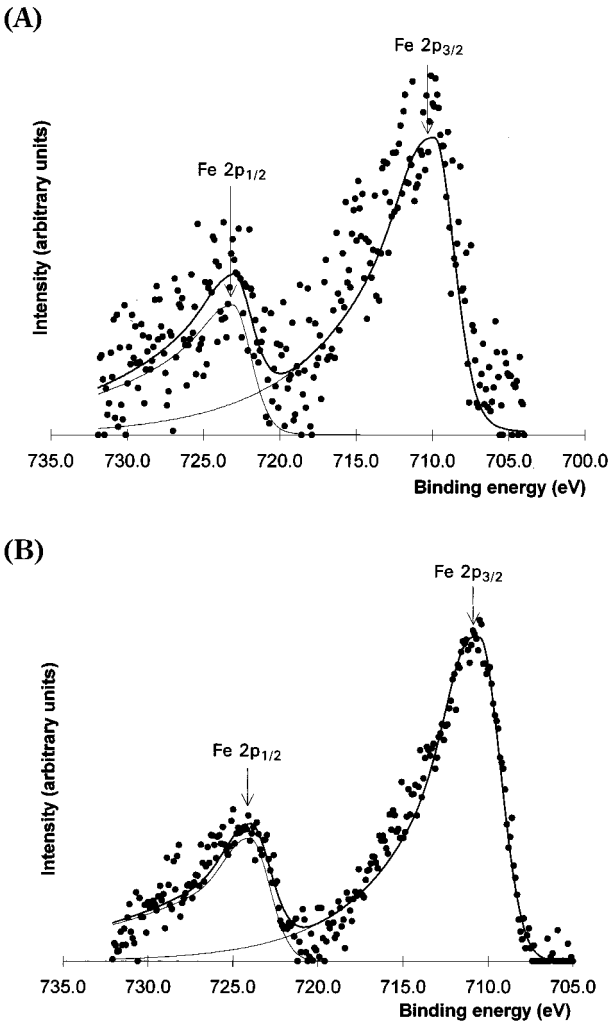

FIGURE 3. XPS spectra of Fe2p region of *Sargassum* biomass exposed to (A) Fe(II) sulfate solution and (B) Fe(III) sulfate solution.

band to lower frequencies. This shift is typical for the complexation of the carbonyl group by dative coordination (*22*) with Ca and/or Fe. Another shift was observed from 1219 cm^{-1} to higher frequencies, corresponding to the complexation of the oxygen from the carbonyl C−O bond. The frequencies corresponding to the C═O and C−O bond stretching in protonated, Ca-, Fe(II)-, Fe(III)-, and combinations of Ca/Fe-loaded materials are given in Table 2 as well as the differences between C═O and C−O band frequencies. The decrease in the distance between the two peaks in Ca and/or Fe complexed biomass types as compared to the protonated biomass reveals the chelating character of the ion complexation to the carboxyl group in the biomass.

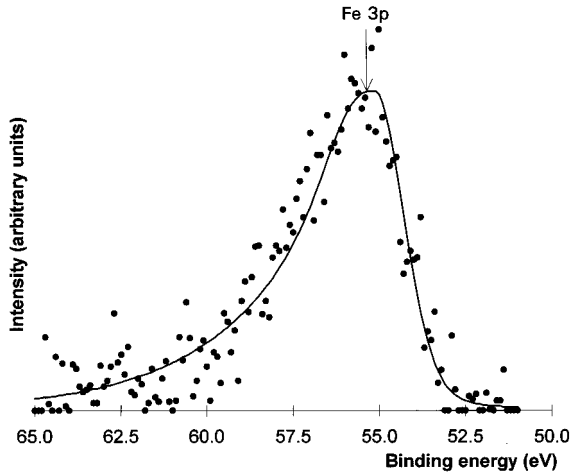

FIGURE 4. XPS spectra of Fe3p region of *Sargassum* biomass exposed to Fe(II) sulfate solution.

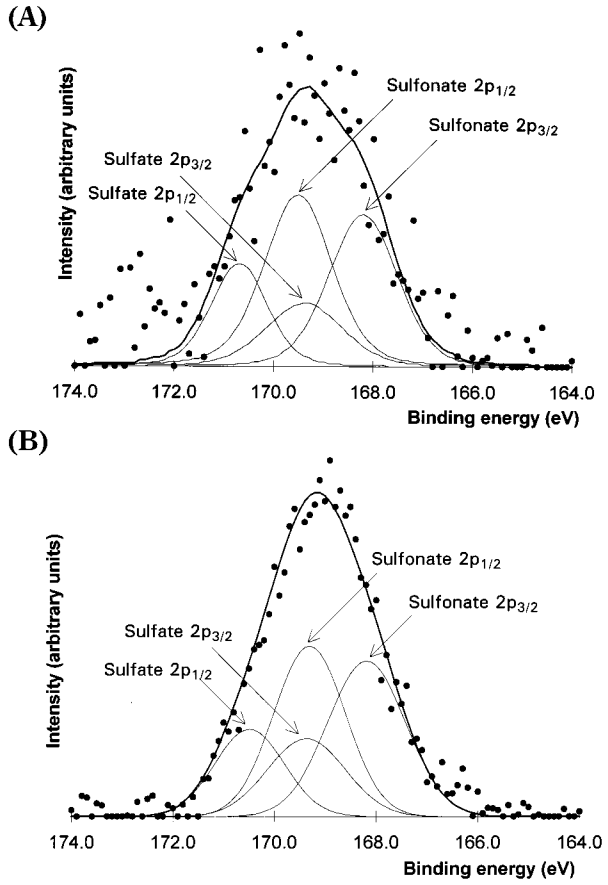

FIGURE 5. XPS spectra of S2p region of *Sargassum* biomass, exposed to (A) Fe(II) sulfate solution and (B) Fe(III) sulfate solution.

Absorbance peaks around 1361 and 1160 cm^{-1}, corresponding to asymmetric and symmetric stretching of SO_3 bonds in sulfonic acids, can be seen in the IR spectrum of protonated biomass. While these peaks present approximately the same frequency for Ca- or Fe(II)-complexed biomass, they are shifted to higher frequencies for biomass exposed to Fe(III) solution (1396 and 1224 cm^{-1} for Fe(III) in protonated biomass and 1385 and 1210 cm^{-1} for Fe(III) in previously Ca-loaded biomass). This can be due to the Fe(III) complexation to sulfonate groups in the biomass; substituents with higher electronegativities reduce resonance contributions from polar forms which result in stiffer S═O bonds and higher frequencies (*23*). Moreover, the complexation of Fe(III) is probably with sulfur, since it is anticipated that coordination through this element will shift the SO stretching bands to higher frequencies (*10*).

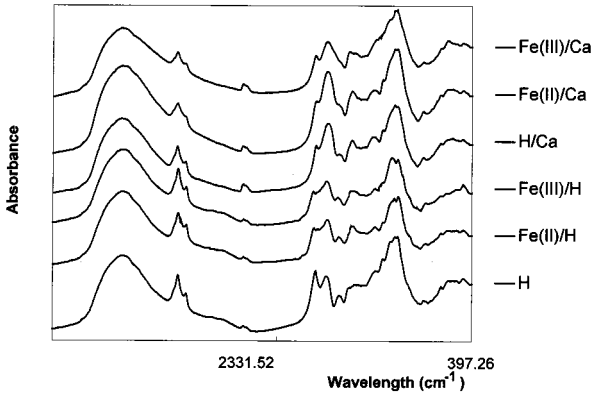

FIGURE 6. FTIR spectra of metal biosorption by *Sargassum* biomass.

TABLE 2: Carboxyl Stretching Frequencies for Different Forms of *Sargassum* Biomass

forms of *Sargassum* biomass	ν (C═O)	ν (C—O)	Δ (C═O − C—O)
protonated	1738.61	1219.63	512.98
Fe(II) in protonated	1639.66	1390.60	249.06
Fe(III) in protonated	1642.09	1396.82	245.27
Ca-loaded	1633.80	1424.23	209.57
Fe(II) in Ca-loaded	1636.98	1422.01	214.97
Fe(III) in Ca-loaded	1636.52	1431.89	204.63

Discussion

Many types of seaweeds have been described as ion-exchanger systems, the cell wall being an important part of the plant tissue in the metal uptake (*24*−*26*). The main functional groups proposed for the metal uptake are carboxyl, sulfydryl, and hydroxyl, mainly those from polyssacharidic material which constitutes most of the cell wall. In *Sargassum* and other Phaeophyceae algae, the thallus is basically formed by a fibrous cellulosic skeleton which contains a mucilaginous matrix of extracellular polyuronic acid (alginate) as well as sulfated glucurono-xylo-fucane (fucoidan) (*27*). There may be some variations in the polysaccharide content of seaweeds in general due to the seasonal changes, depth of growth in the sea, and some intrinsic characteristics of the different species (*28*). Still, a general constitution of *Sargassum* biomass is approximately 7−14% of alginate, less than 1% mannitol, 4% fucoidan, and high cellulose content (*29*).

As observed in the electron micrograph of *Sargassum* biomass exposed to iron solution (Figure 1), the metal is deposited mainly in the cell wall, but some Fe could also be detected in the cytoplasm material. Since the biomass was not previously preserved and thus suffered from rapid desiccation, most of its material, and especially the mucilaginous component of the cell wall, could have been mixed into the cytoplasmatic contents of the cell. This would explain the deposition of Fe also inside the cell, although to a lesser extent. Other types of constituents usually present in the cytoplasm, such as proteins, could provide functional groups for metal uptake to occur.

The deposition of cadmium in the cell wall of the macroalga *Ulva lactuca* was also observed by Webster and Gadd (*26*). While the metal was found in all of the areas of the cell, changes in the chemical composition, observed by EDS analysis, were apparent only in the cell wall of the thallus. The authors proposed that an ion-exchange mechanism occurred in the algal cell wall, the calcium present in polysaccharide subunits being replaced by cadmium. The

cell wall of *Sargassum* cells was also established as the main part of the cell involved in sequestering gold from solution (*5*). However, intracellular gold deposition was also observed by the TEM/EDS analysis, showing the permeability of the algal tissue to the metal.

Although care was taken in the present studies to avoid any natural oxidation of the ferrous iron present in the biomass, the results of the XPS analysis of metal-loaded *Sargassum* biomass showed the presence of both Fe(II) and Fe(III) in the ferrous iron-exposed biomass (Figure 3A). Ferrous iron is easily oxidized by air, and just the manipulation of the sample for the XPS analysis could be enough to produce a partial oxidation. An attempt to "clean" the very surface of the particles by sputtering by Ar bombardment was unsuccessful since this approach is known to reduce forms of more oxidized Fe (*30*). This could lead to a misinterpretation of the results, and thus the sputtering was not applied to any of the samples. However, the Fe(3p) spectrum of Fe(III)-exposed biomass showed that only ferric iron was present in the sample (Figure 4). This indicates that ferric iron is deposited as such, without being reduced by the biomass. It has been demonstrated that certain species of Fe(III) can undergo a reductive process in the presence of organic matter (*31*). A typical example of an organic substance known to reduce Fe(III) precipitates is fulvic acid (*32*).

A reduction mechanism of gold was proposed by Kuyucak (*5*) when the metal was sequestered by *Sargassum* biosorbent from a gold chloride solution. Tannin was the component suggested to play a role in the reduction of gold due to its strong reducing action. The presence of elemental gold was detected by the determination of ionization energies for Au-(4f). However, two major peaks were observed in the XPS spectrum for the biomass exposed to $AuCl_4$, indicating the presence of more than one type of gold. The second type of gold form was suggested to be mononuclear compounds formed with functional groups in the biomass, probably with the hydroxyl of carboxylic acid groups.

Alginate seems to play a key role in the uptake of cations by brown algae, the carboxyl groups from polyuronic acids being the most important ones. The modification of carboxyl groups by esterification with acidic methanol resulted in a significant decrease in the binding of Cu and Al but in a slight increase in Au binding by five different algae (*33*). The decrease in sorption was more pronounced for Al, which as a hard metal is expected to bind preferably to hard sites such as carboxyl groups, whereas Cu as a softer metal may rather bind to nitrogen or sulfur-containing groups. The binding of the negatively charged Au complex increased probably due to a decrease in the negative surface charge. Fourest and Volesky (*34*) investigated the binding of H, Cd, and Pb by alginic acid and *Sargassum fluitans* biomass before and after modification of the carboxyl groups using acidic methanol or propylene oxide. A linear correlation between the binding capacity for Cd and the content of weak acidic groups (probably carboxylate) resulting from different degrees of blocking was noted. A 48-h treatment with propylene oxide resulted in a ~90% reduction of Cd binding and a ~80% reduction of Pb binding as well as a 80% reduction of titrable weak acidic (carboxylic) groups. This indicated that a majority of the metal was bound by carboxyl groups.

The carboxyl group of alginate is also suggested here as a key component for Fe uptake by *Sargassum* biomass, especially at pH 4.5. It is expected that at this pH, most of the carboxylic groups would be available for ion exchange (the pK_a of carboxylic acids in biomolecules is reported as being between 3 and 5) (*35*).

One way of confirming the role of carboxylic groups in the uptake of iron would be by interpreting the O and C regions of the XPS spectrum. However, this is a much more complicated approach due to the many possible components of the biomass containing C and O which may make the spectrum interpretation rather complex and difficult. Another approach is the analysis of the biomass by FTIR. This was the strategy used by Fourest and Volesky (*7*) to investigate the mechanism of cadmiun biosorption by *Sargassum* biomass. The protonated biomass was used as a free biosorbent control since the presence of cations from the seawater (Na, K, Mg, Ca, for example) could interfere in the IR peak analysis. This approach allowed the identification of two absorbance peak shifts and led to the conclusion on the participation of carboxyl groups in the metal uptake.

FTIR analysis was conducted with metal-loaded biomass in order to identify groups involved in the biosorption of cations (Figure 6). As in the case of the Cd uptake, carboxyl groups were found to be involved in the Ca and Fe uptake, independently of the Fe form present. It was possible to identify two absorbance peak shifts in the FTIR spectra which are characteristic of coordination compounds between carboxyl groups and the cations used. The distance between these two peaks (Δ) is related to the relative symmetry of the carboxyl group and reflects the nature of the coordination compound. Protonated compounds exhibit the highest Δ, followed by the unidentate complexes. This value is significantly lower with chelating (bidentate) complexes. Bridging complexes display higher values of Δ as compared to chelating ones but close to ionic values (*10*). The data obtained for different forms of cation−biomass complexes (Table 2) showed that all of the ion complex forms obtained with Ca or Fe exposure have lower Δ values than that for protonated biomass, suggesting the chelating character of the metal biosorption onto carboxyl groups. The overall structure of the carboxyl group bound to metal (M) in a chelating form would be as suggested by Nakamoto (*10*).

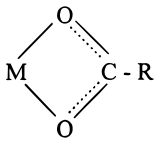

The protonated biomass exposed to Fe(II) and Fe(III) solutions showed higher Δ values. This could be explained by the partial loading of the sites available: for protonated biomass, the pH of the solution decreased as the ion exchange occurred, thus leading to a lower uptake of metals from the solution (*7*, *36*), and the contribution of the remaining protonated sites to the overall FTIR spectra would be to reduce the shifts for C═O and C—O stretching vibrations.

The FTIR spectra obtained for the biomass previously exposed to ferric iron solutions also show shifts in the frequencies of the symmetric and asymmetric stretching of SO_3. This group is mainly present in sulfonic acids of polysaccharides, such as fucoidan, in the biomass. The possible complexation of divalent metals to sulfonate groups was not observed for Cd biosorption by *Sargassum* in previous studies (*7*), and in the present work, the FTIR analysis showed no major difference in the frequencies for that group when the biomass was exposed to Ca or Fe(II) solutions. This suggests that this group could be of some importance in the overall uptake of trivalent metal ions such as Fe(III). The confirmation of this hypothesis could come again from the XPS spectra. However, the analysis of the S2p XPS spectra (Figure 5) showed that both sulfate and sulfonate groups are present in both Fe(II)- and Fe(III)-exposed biomass samples with similar binding energy values (Table 1). The only difference observed was in relation to the FWHM for $S2p^3/_2$ peak which was broader in the Fe(III)-exposed biomass than in the Fe(II)-exposed biomass. The presence of sulfate groups

in both XPS S2p spectra may be due to some residual sulfate from the Fe salt used in the experiments.

The XPS technique was also applied in studies of the iron valence in metal-containing proteins (*12*). The ionization energies for several bacterial ferrodoxins were obtained and compared in order to obtain information about their oxidation states and possible configuration. The author observed that the Fe(III) bound to soft ligands (sulfur) exhibited values of about 710.00 ± 0.5 eV whereas the values for Fe(II) were about 708.00 ± 0.5 eV. If Fe(III) is bound to hard ligands (e.g., oxygen), the ionization energy values were shown to be 711.00 ± 0.5 eV, where Fe(III) is tetrahedrally surrounded by oxygen. This information led to proposing a cluster model for the arrangement of Fe in the ferrodoxins studied, where Fe would be present in only one oxidation state.

Several studies of metal deposition in biological tissues as a means of staining for electron microscopy purposes have been carried out in order to investigate the mechanism and possible selectivity of the metals toward different biomolecules. This information can contribute to understanding of the Fe biosorption mechanism by *Sargassum* biomass. It seems that a variety of macromolecules which possess negatively charged hydroxyl, carboxyl, sulfate, and phosphate groups have the ability to chelate with iron. However, iron binding may not be totally a function of the charge present in the molecule. The solution pH is an important factor in the iron binding to molecules; at low pH (∼1.8) it is primarily due to the availability of free ferric anions to the phosphate, sulfate, and certain groups with low p*K* values (*37*). It is important to note that a change in the pH results in an immediate alteration of the electrostatic properties of the cell components which, in turn, induces conformational changes. Therefore, increased or decreased binding cannot be completely explained by a simple change in the electrostatic properties of the cell components; other factors, such as accessibility and conformation, are also important (*1*).

Conformation and site size are characteristics also related to the affinity of polysaccharides such as alginate to ions. Calcium-induced gel formation of seaweed alginate is due to the physical binding of Ca ions to guluronate residues based on a charge-to-charge interaction between the positive charge from Ca ions and the negative charge of the guluronic acid carboxyl groups. The size of the Ca ion allows it to fit into the space formed by guluronic residues between antra e intermolecules of seaweed alginates (*38*, *39*). This is the basis of the Rees alginate "egg box model" (*40*). Lee et al. (*41*) found that acetylation (modification of the degree of ionization by reduction of the net negative charge of the polymers) dramatically affects the metal-induced precipitation of alginates. The presence of the acetyl group decreased the ability of the polymer to bind with Ca but increased the ability to bind with ferric ion. Although the ionic effect of the carboxyl group is unlikely to be dramatically influenced, acetylation of alginate probably disturbs the basic relationships between the polymer and Ca or divalent ions by sterically hindering the binding of these ions to the polymer. They also suggested that the steric changes in the acetylated alginate molecule could favor a higher affinity for the polymer for ferric ions.

This study provides evidence of the participation of carboxyl groups in the uptake of iron ions, both Fe(II) and Fe(III), and of sulfonate groups in the uptake of Fe(III) by *Sargassum* biomass. As in the uptake of Cd by this seaweed, the carboxyl groups would be mainly those present in alginate molecules and the fucoidan polysaccharide would provide the sulfonate groups. The solution pH plays an important role in the availability of these groups for an ion-exchange mechanism and in the conformational structure of the molecule. The metal ion could be bound by the particular sites depending on its ionic size and the accessibility of the sites for its deposition. Other instrumental analysis such as EPR (electron paramagnetic resonance) could provide more information on the particular conformation of the sites around the metal ion, and a computational molecular modeling approach could help in visualizing the structure of the molecule and especially the environment around the sequestered ion.

Acknowledgments

The Brazilian CAPES Scholarship support to M.M.F. is gratefully aknowledged. Mr. N. Xanthopoulos (Laboratoire de Metallurgie Chimique, EPFL, Switzerland) contributed in the XPS analyses. Mr. Graeme Auchterlonie (Center for Microscopy and Microanalysis, University of Queensland, Australia) expertly helped with the TEM/EDS analyses.

Literature Cited

(1) Hayat, M. A. *Principles and Techniques of Electron Microscopy − Biological Applications*; CRC Press: Boca Raton, FL, 1989; pp 221, 285−290.
(2) Shumate, S. E. I.; Strandberg, G. W. In *Comprehensive Biotechnology*; Moo-Young, M., Ed.; Pergamon Press: New York, 1985; Vol. 4, pp 235−247.
(3) Volesky, B.; Holan, Z. R. *Biotechnol. Prog.* **1995**, *11*, 235−250.
(4) Kratochvil, D.; Volesky, B. *Trends Biotechnol.* **1998**, *16*, 291−300.
(5) Kuyucak, N.; Volesky, B. *Biorecovery* **1989**, *1*, 219−235.
(6) Schiewer, S.; Volesky, B. *Environ. Sci. Technol.* **1996**, *30*, 2921−2927.
(7) Fourest, E.; Serre, A.; Roux, J.-C. *Toxicol. Environ. Chem.* **1996**, *54*, 1−10.
(8) Figueira, M. M.; Volesky, B.; Ciminelli, V. S. T. *Biotechnol. Bioeng.* **1997**, *54*, 344−350.
(9) Kratochvil, D.; Volesky, B. *Water Res.* **1998**, *32*, 2760−2768.
(10) Nakamoto, K. *Infrared and Raman Spectra of Inorganic and Coordination Compounds*; John Wiley & Sons: New York, 1997; p 60.
(11) Clark, D. T. In *Handbook of X-ray and Ultraviolet Photoelectron Spectroscopy*; Briggs, D., Ed.; Heyden & Son: London, U.K., 1977; pp 211−247.
(12) Leibfritz, D. *Angew. Chem., Int. Ed. Eng.* **1972**, *11*, 232−234.
(13) Brizzolara, R. A.; Boyd, J. L.; Tate, A. E. *J. Vac. Sci. Technol., A* **1997**, *15*, 773−778.
(14) Vogel, I. A. *Quantitative Inorganic Analysis*; Longman Group Ltd.: London, U.K., 1961; pp 304−309.
(15) Spurr, A. R. *J. Ultrastruct. Res.* **1969**, *26*, 31−43.
(16) Hayat, M. A. *Principles and Techniques of Electron Microscopy − Biological Applications*; CRC Press: Boca Raton, FL, 1989; pp 72−73.
(17) Stumm, W.; Morgan, J. J. *Aquatic Chemistry*; Wiley-Interscience: New York, 1981; pp 779−781.
(18) McIntyre, N. S.; Zetaruk, D. G. *Anal. Chem.* **1977**, *49*, 1521−1529.
(19) Moulder, J. F.; Stickle, W. F.; Sobol, P. E.; Bomben, K. D.; Chastain, J. *Handbook of X-ray Photoelectron Spectroscopy*; Perkin-Elmer Corp. Physical Electronics Division: Minnesota, 1992.
(20) Lindberg, B. J.; Hamrin, K.; Johansson, G.; Gelius, U.; Fahlman, A.; Nordling, C.; Siegbahn, K. *Phys. Scr.* **1970**, *1*, 286−298.
(21) Beamson, G.; Briggs, D. *High-Resolution XPS of Organic Polymers − The Scientia ESCA300 database*; John Wiley & Sons: Chichester, U.K., 1992; p 295.
(22) Nakamoto, K. *Infrared and Raman Spectra of Inorganic and Coordination Compounds*; J. Wiley & Sons: New York, 1986; p 231.
(23) Colthup, N. B.; Daly, L. H.; Wiberley, S. E. *Introduction to Infrared and Raman Spectroscopy*; Academic Press: San Diego, CA, 1990; p 547.
(24) Kloareg, B.; Demarty, M.; Mabeau, S. *J. Exp. Bot.* **1987**, *38*, 1652−1662.
(25) Crist, R. H.; Martin, J. R.; Carr, D.; Watson, J. R.; Clarke, H. J.; Crist, D. R. *Environ. Sci. Technol.* **1994**, *28*, 1859−1866.
(26) Webster, E. A.; Gadd, G. M. *BioMetals* **1996**, *9*, 241−244.
(27) Percival, E.; McDowell, R. H. *Chemistry and Enzymology of Marine Algal Polysaccharides*; Academic Press: London, U.K., 1967; pp 99−126.
(28) Percival, E. In *The Carbohydrates*; Pigman, W., Horton, D., Eds.; Academic Press: New York, 1970; IIB, pp 537−538.
(29) Dodge, J. D. *The Fine Structure of Algal Cells*; Academic Press: London, U.K., 1973; pp 14−45.

(30) Brundle, C. R.; Chuang, T. J.; Wandelt, K. *Surf. Sci.* **1977**, *68*, 459−468.
(31) Vile, M. A.; Wieder, K. R. *Water, Air, Soil Pollut.* **1993**, *69*, 425−441.
(32) Deng, Y.; Stumm, W. *Aquat. Sci.* **1993**, *55*, 1015−1621.
(33) Gardea-Torresdey, J. L.; Becker-Hapak, M. K.; Hosea, J. M.; Darnall, D. W. *Environ. Sci. Technol.* **1990**, *24*, 1372−1378.
(34) Fourest, E.; Volesky, B. *Environ. Sci. Technol.* **1996**, *30*, 277−282.
(35) Bower, V. E.; Bates, R. G. In *Handbook of Analytical Chemistry*; Meites, L., Ed.; McGraw-Hill: New York, 1963; pp 1.20−1.27.
(36) Schiewer, S.; Volesky, B. *Environ. Sci. Technol.* **1995**, *29*, 3049−3058.
(37) Sprumont, P.; Musy, J.-P. *Histochemie* **1971**, *26*, 228−237.
(38) Morris, E. R.; Rees, D. A.; Thom, D. *Carbohydr. Res.* **1978**, *66*, 145−154.
(39) Morris, E. R.; Rees, D. A. *J. Mol. Biol.* **1980**, *16*, 88−91.
(40) Rees, D. A. *Biochem. J.* **1972**, *126*, 257−282.
(41) Lee, J. W.; Ashby, R. D.; Day, D. F. *Carbohydr. Polym.* **1996**, *29*, 337−345.

Received for review October 29, 1998. Revised manuscript received February 24, 1999. Accepted March 1, 1999.

ES981111P